

# WatchPed: Pedestrian Crossing Intention Prediction Using Embedded Sensors of Smartwatch

Jibran Ali Abbasi, Navid Mohammad Imran, and Myounggyu Won

Connected Smart Sensor Systems (CS<sup>3</sup>) Laboratory  
 Department of Computer Science  
 University of Memphis  
 {jaabbasi, nimran, mwon}@memphis.edu

## Abstract

The pedestrian intention prediction problem is to estimate whether or not the target pedestrian will cross the street. State-of-the-art approaches heavily rely on visual information collected with the front camera of the ego-vehicle to make a prediction of the pedestrian’s intention. As such, the performance of existing methods significantly degrades when the visual information is not accurate, *e.g.*, when the distance between the pedestrian and ego-vehicle is far, or the lighting conditions are not good enough. In this paper, we design, implement, and evaluate the first pedestrian intention prediction model based on integration of motion sensor data gathered with the smartwatch (or smartphone) of the pedestrian. A novel machine learning architecture is proposed to effectively incorporate the motion sensor data to reinforce the visual information to significantly improve the performance in adverse situations where the visual information may be unreliable. We also conduct a large-scale data collection and present the first pedestrian intention prediction dataset integrated with time-synchronized motion sensor data. The dataset consists of a total of 128 video clips with different distances and varying levels of lighting conditions. We trained our model using the widely-used JAAD and our own datasets and compare the performance with a state-of-the-art model. The results demonstrate that our model outperforms the state-of-the-art method particularly when the distance to the pedestrian is far (over 70m), and the lighting conditions are not sufficient.

## Introduction

The pedestrian intention prediction problem is to forecast whether or not the target pedestrian will cross the street over a short time horizon (Zhao et al. 2021). Accurately predicting the pedestrian’s intention is of great importance for assuring traffic safety (Quintero et al. 2017). The safety of advanced driver assistance systems (ADAS) for human-driven and autonomous vehicles can be boosted with the capacity of estimating the pedestrian’s crossing behavior (Razali, Mordan, and Alahi 2021). By providing early warnings, the driver or the autonomous vehicle itself can earn an ample time for responding to unexpected situations to prevent accidents (Cadena et al. 2022). Developing techniques for effective prediction of pedestrian’s intention is one of the most important requirements to achieve the level-4 autonomy especially in urban environ-

ments where autonomous vehicles frequently interact with pedestrians (Yang et al. 2022).

There are largely two streams of research on pedestrian intention prediction: methods to predict the pedestrian’s intention by estimating the trajectory of the pedestrian (Alahi et al. 2016; Lee et al. 2017; Bartoli et al. 2018; Gupta et al. 2018; Sadeghian et al. 2019), and machine learning approaches to directly estimate the pedestrian’s intention based on different types of input features (Neogi et al. 2017; Saleh, Hossny, and Nahavandi 2019; Gujjar and Vaughan 2019). Numerous works have demonstrated that the trajectory-based approaches can effectively identify the pedestrian’s intention to cross the street. However, since those methods require the motion history of the pedestrian, in some real-world scenarios, *e.g.*, pedestrians are just standing on a sidewalk to find a chance to cross the street (*i.e.*, there does not exist the past motion track), the trajectory-based solutions fail to work (Razali, Mordan, and Alahi 2021; Zhao et al. 2021). In this paper, we focus on a more general approach that makes a pedestrian intention prediction directly based on the fusion of different types of input features.

Early machine learning-driven approaches were based on convolutional neural networks (CNNs) (Rasouli, Kotseruba, and Tsotsos 2017). Subsequently, to enhance the precision of pedestrian’s intention prediction, spatial and temporal correlations between video frames were incorporated by adopting recurrent neural networks (Kotseruba, Rasouli, and Tsotsos 2020; Lorenzo et al. 2020; Rasouli et al. 2019). Different types of input features were fused to achieve better performance such as pedestrian poses, bounding boxes, ego-vehicle information, and semantic segmentation maps (Fang and López 2018; Piccoli et al. 2020; Rasouli, Kotseruba, and Tsotsos 2020; Rasouli et al. 2020; Rasouli, Rohani, and Luo 2021). Latest works integrate additional input features related to the road geometry and surrounding people (Yang et al. 2022), and there are some works that utilize graph convolutional networks (GCNs) to better represent the input features to improve performance (Cadena et al. 2022).

One common aspect of most of the existing approaches is that a prediction of the pedestrian’s intention is made by heavily relying on visual information obtained from the front camera of the ego-vehicle. As such, the prediction ac-

curacy can intensely degrade when the visual information is not accurate enough, *e.g.*, in situations where the distance between the pedestrian and ego-vehicle is far, or the lighting conditions are not sufficient.

To address the inherent limitation of state-of-the-art approaches, we present WatchPed: a pedestrian intention prediction model designed to reinforce the visual information by augmenting with motion sensor data gathered with the embedded sensors of smartwatch of the pedestrian. A novel neural network architecture is created that effectively incorporates the motion sensor data with the visual information to make a more precise prediction of the pedestrian’s intention. The architecture consists of (1) the vision branch that processes the local and global visual context information, (2) the non-vision branch that consolidates non-visual features including the ego-vehicle speed, the bounding box of the pedestrian, and the pose information of the pedestrian, and (3) the sensor branch that incorporates the pedestrian’s motion sensor data in the decision making process. Fusion of various input features is performed to significantly improve the performance even under the circumstances where the visual information may be unreliable. Furthermore, we also perform a large-scale data collection and present the first pedestrian intention prediction dataset integrated with time-synchronized motion sensor data. The proposed dataset consists of a total of 128 video clips with varying distances and different levels of lighting conditions, which is ideally suited for development of pedestrian intention prediction solutions based on motion sensor data. We trained our model using both the widely-adopted JAAD dataset as well as our own dataset and compared the performance with a state-of-the-art method (Yang et al. 2022). We demonstrate that our approach significantly improves the performance especially when the distance between the pedestrian and ego-vehicle is large, and lighting conditions are not good enough.

The following is a summary of our contributions:

- We present the first pedestrian intention prediction model integrated with motion sensor data collected with the embedded sensors of smartwatch of the pedestrian to address the inherent limitation of state-of-the-art approaches caused by excessive reliance on visual information to perform prediction.
- We perform a large-scale data collection and introduce the first pedestrian intention dataset that consists of visual, non-visual, and time-synchronized motion sensor data of pedestrians.
- We conduct an extensive experiment to demonstrate that our model outperforms a state-of-the-art approach especially when the distance between the pedestrian and ego-vehicle is very far, and/or lighting conditions are not sufficient.

This paper is organized as follows. We review state-of-the-art pedestrian intention prediction methods in the Related Work section, followed by the details of our dataset in the Proposed Dataset section. We then present the design of the architecture of the proposed model in the Proposed Approach section. The results of our experimental study are

presented in the Experimental Results section. We then conclude in the Conclusion section.

## Related Work

The pedestrian intention prediction problem is to forecast whether or not a given pedestrian will cross the road (Kotseruba, Rasouli, and Tsotsos 2021). Numerous machine learning architectures based on manifold data modalities have been proposed to solve the problem. Some early efforts capitalized on static traffic scenes and pedestrian walking actions represented by CNNs to predict the pedestrian’s intention (Rasouli, Kotseruba, and Tsotsos 2017). The performance limitations due to stationary input features were amended by utilizing a sequence of frames (Lorenzo et al. 2020; Piccoli et al. 2020). Additionally, multimodal methods were studied to incorporate different types of information such as trajectories of the pedestrian (Rasouli, Kotseruba, and Tsotsos 2020), body parts of the pedestrian (Cadena et al. 2019), and interactions between pedestrians and other agents (Liu et al. 2020).

Numerous variants of existing approaches have been studied. Generative models were used to predict scene representations more effectively (Gujjar and Vaughan 2019; Chaabane et al. 2020). Singh and Suddamalla incorporated both the global (*i.e.*, visual features of different objects surrounding the pedestrian) and local context information (*i.e.*, visual features of the target pedestrian) (Singh and Suddamalla 2021). Chen *et al.* considered the elements of the ego-scene to provision future context for motivation (Chen, Tian, and Ding 2021). Lorenzo *et al.* proposed a self-attention alternative based on transformer architecture which effectively fused video and pedestrian kinematic data (Lorenzo et al. 2021). Razali *et al.* designed a neural network based on a 5-block ResNet-50 to generate a map for predicting the probability for each pixel that belongs to a pedestrian (Razali, Mordan, and Alahi 2021). Yang *et al.* adopted a 3D CNN to capture the key behavioral information before the pedestrian crosses the street instead of relying on the skeleton features which may not be accurate if the distance between the pedestrian and vehicle is far (Yang et al. 2021). Zhao *et al.* proposed a method that combines the complementary strengths of multi-modal data to improve the performance (Zhao et al. 2021). The vision transformer was utilized to process sequential data more effectively. Cadena *et al.* proposed a modified GCN-based model by adding the contextual information such as the vision information about the environment (Cadena et al. 2022). Zhang *et al.* utilized CCTV videos to effectively capture the key points of the pedestrian body (Zhang et al. 2021). Yang *et al.* proposed a hybrid model that is designed to fuse different features from various input sources including both the non-visual and visual information (Yang et al. 2022).

Despite decent performance for predicting the pedestrian’s intention, existing works have vital limitations that need immediate attention before being adopted as a key safety component of autonomous vehicles. Significant dependence on visual information makes them hard to predict the pedestrian’s intention when the distance between

the pedestrian and ego-vehicle is far. The performance further degrades when the lighting conditions are not enough. Yet, even a slim glitch is not permissible as far as safety is concerned. Therefore, our approach is designed to achieve the goal of maximizing pedestrian safety in such circumstances where the visual information may not be accurate by incorporating with the motion sensor data of the pedestrian collected with the pedestrian’s smartwatch in performing pedestrian intention prediction. Moreover, a novel pedestrian intention dataset which contains time-synchronized pedestrian motion sensor data has been created and publicized.

## Proposed Dataset

### State-of-the-Art Pedestrian Intention Dataset

One of the first publicly available pedestrian intention dataset is the Joint Attention in Autonomous Driving (JAAD) dataset (Rasouli and Tsotsos 2018). It contains 346 short video snippets recorded with a dashboard camera under different weather conditions. Numerous solutions for pedestrian intention prediction were evaluated with the JAAD dataset. Another widely used dataset is Trajectory Inference using Targeted Action priors Network (TITAN) (Malla, Dariush, and Choi 2020). Compared to JAAD, TITAN is a large-scale dataset with fine-grained labeling. It consists of 10 hours of video (700 short clips) containing 8,592 unique pedestrians recorded in Tokyo, Japan. Stanford-TRI Intent Prediction (STIP) is another well recognized pedestrian intention dataset (Liu et al. 2020). A unique aspect of the STIP dataset is that the video was recorded using three cameras covering left, right, and front of the ego-vehicle. By incorporating multiple camera angles, pedestrian intention prediction could be performed more effectively. The authors of the JAAD dataset have released a new version dubbed as Pedestrian Intention Estimation (PIE) (Rasouli et al. 2019). PIE was recorded in Toronto, Canada. Compared with their older version JAAD, PIE contains more labeling and includes more information on the ego-vehicle motion.

### Our Dataset

To build our dataset, video recording has been carried out in the streets in XX, YY, ZZ. Common pedestrian-crossing scenarios were considered where there is a pedestrian wearing a smartwatch, and a vehicle is moving toward the pedestrian. The dashboard camera of the vehicle was used to capture the visual information of the pedestrian. A total of 128 HD video snippets were recorded consisting of a total of 61,679 annotated frames of pedestrians. Each 30-fps video clip has a running time between 10 to 30 seconds. The vehicle speed was recorded using the iPhone Timestamp Camera App once every 30 frames (*i.e.*, every second). The Sensor Box App of a smart watch was used to record 50 accelerometer and gyroscope readings along with the corresponding timestamps per second. The full dataset is available at <https://XX>.

Our dataset is unique compared to state-of-the-art datasets in several aspects. First, video clips were strategically



Figure 1: Examples of different types of input features provided in our dataset.

recorded in different scenarios with varying distances between the pedestrian and ego-vehicle. Similarly, our dataset consists of video snippets recorded under different lighting conditions (*i.e.*, sunny, night, cloudy, and rainy conditions). A more dominant aspect of our dataset is that it consists of different types of time-synchronized input features including visual, non-visual, and motion sensor data. To the best of our knowledge, our dataset is the first of its kind that is integrated with time-synchronized motion sensor data collected with the smartwatch of pedestrians.

### Data Processing and Labeling

All data were archived in the style of the JAAD dataset (Rasouli and Tsotsos 2018). More specifically, each video frame is annotated with the bounding box and pose information of the pedestrian. Additionally, behavioral tags including actions such as walking, standing, crossing, looking, *etc.* are provided as annotations for each pedestrian per frame. The attributes of each pedestrian including age, gender, direction of motion, clothing, crossing location, *etc.* are also provisioned for each frame. Each video is annotated with the weather conditions and time of day information, and visible objects in a scene such as crosswalks, stop signs, traffic lights, *etc.* are also provided as annotations.

The accelerometer and gyroscope data collected with the smartwatch of the pedestrian are included in our dataset as the motion sensor data. The motion sensor data are time-synchronized with the corresponding video frames. More precisely, GPS-based timestamps were used to implement time synchronization at a precision of 0.001 second.

To generate the bounding boxes of each pedestrian (*e.g.*, see Fig. 1(a)), the YOLOv4-1280 model (with DeepSort object tracking) (Wojke and Bewley 2018) was used. This model is quite accurate in capturing bounding boxes when the distance between the pedestrian and ego-vehicle is close enough. However, it was observed that the model frequently failed to generate bounding boxes as the distance increased.

To calibrate the YOLOv4-1240 model and successfully generate a bounding box for each and every frame, we used a linear interpolation method. More specifically, the Label Studio was used to manually produce bounding boxes that were not captured by the YOLOv4-1240 model. A sufficient number of bounding boxes were produced intermittently between frames. The gaps (*i.e.*, frames with no bounding boxes between manually captured bounding boxes) were filled in through a linear interpolation method.

As we mentioned, each video frame is annotated with the pedestrian pose information (see Fig. 1(b)). The OpenPose

model (Cao et al. 2017) was used to capture the pose information. The model reads each frame and generates 18 key points for each pedestrian it detects. It was observed that the model effectively captured the pedestrian pose information when the pedestrian was located close to the ego-vehicle. However, as the distance increased, we encountered situations where non-human objects were detected as humans and the key points for them were generated. To fix this problem, we utilized the bounding box that was created in the previous step. More specifically, we purged the noisy pose information by incorporating only the key points that were within the pedestrian bounding box. Still, despite our algorithm to enhance the precision of the OpenPose model, the model completely failed to generate the key points when the distance was very far. For those frames, annotations of the pedestrian pose information were not provided.

Our dataset also provides both the local and global context by closely following the idea presented in (Yang et al. 2022). The local context represents the visual features of the pedestrian. It comprises of a sequence of  $(224 \times 224)$  pixels) RGB images of the surroundings of the pedestrian (see Fig. 1(c)). The global context conveys the visual features of the objects in the video that can be used as a clue to infer the pedestrian-crossing activity. Pixel-level semantic masks were used to extract the global context from the video by classifying, localizing, and labeling those objects (see Fig. 1(d)). DeepLabV3 (Chen et al. 2017) pre-trained with the Cityscapes Dataset (Cordts et al. 2016) was used to extract the semantic masks for the relevant objects. The extracted semantic segmentations were represented as  $(224 \times 224)$  pixels) RGB images.

## Proposed Approach

This section presents an overview of the proposed model, followed by the details of the model architecture.

### Overview

Fig. 2 displays an overview of the proposed approach. An ego-vehicle makes a prediction of the pedestrian’s intention using a machine learning model trained with three different types of input feature vectors extracted from visual, non-visual, and motion sensor data, respectively. As shown in Fig. 2, the visual and non-visual data are gathered using the dashboard camera, and the motion sensor data collected from the smartwatch of the pedestrian are transmitted to the ego-vehicle via V2X (vehicle-to-everything) communication. The visual features include the global and local environmental context. The non-visual features are the ego-vehicle speed, trajectory of the pedestrian (which is obtained based on the bounding box sequence of the pedestrian), and the pose key points of the pedestrian. The motion sensor features contain the sequence of the accelerometer and gyroscope sensor data.

Our goal is to design a neural network architecture for the ego-vehicle to estimate the probability distribution  $\mathcal{P}(A_i^{t+f} | L_i, P_i, C_i, S_i, G, V) \in [0, 1]$  that the target pedestrian  $i$ ’s action  $A_i^{t+f} \in \{0, 1\}$  is to cross the street, where  $t$  refers to the time of the latest frame, and

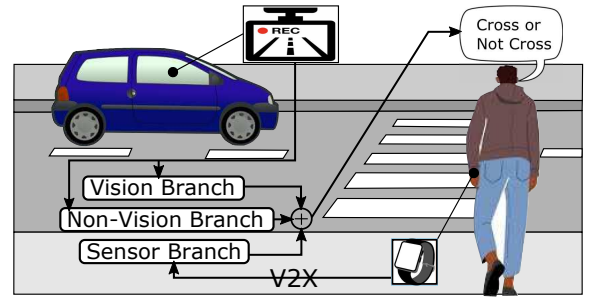


Figure 2: An overview of the proposed pedestrian intention prediction method.

$f$  is the number of frames representing the future time horizon for pedestrian intention prediction. Here,  $L_i = \{l_i^{t-m}, l_i^{t-m+1}, \dots, l_i^t\}$  is the pedestrian  $i$ ’s trajectory which is a sequence of the pedestrian  $i$ ’s bounding box coordinates. More precisely,  $l_i^{t-m} = \{x_{it}^{t-m}, y_{it}^{t-m}, x_{ib}^{t-m}, y_{ib}^{t-m}\}$ , where  $x_{it}^{t-m}, y_{it}^{t-m}$  are the x and y coordinates for the top-left point, and  $x_{ib}^{t-m}, y_{ib}^{t-m}$  are the ones for the bottom-right point.  $P_i = \{p_i^{t-m}, p_i^{t-m+1}, \dots, p_i^t\}$  refers to the pedestrian  $i$ ’s pose information. Each element of  $P_i$  represents a set of 18 2D coordinates for pose joints, *i.e.*,  $p_i^{t-m} = \{x_{i1}^{t-m}, y_{i1}^{t-m}, x_{i2}^{t-m}, y_{i2}^{t-m}, \dots, x_{i18}^{t-m}, y_{i18}^{t-m}\}$ .  $G = \{g^{t-m}, g^{t-m+1}, \dots, g^t\}$  is the sequence of the global context, and  $C_i = \{c_i^{t-m}, c_i^{t-m+1}, \dots, c_i^t\}$  is the sequence of the local context for pedestrian  $i$ .  $S_i = \{s_i^{t-m}, s_i^{t-m+1}, \dots, s_i^t\}$  is the sequence of the motion sensor data for pedestrian  $i$ .  $V = \{v^{t-m}, v^{t-m+1}, \dots, v^t\}$  is the speed of the ego-vehicle.

### Model Architecture

Fig. 3 displays an architecture of the proposed model. It consists of four main branches, *i.e.*, the vision, non-vision, initial fusion, and motion sensor branches. The vision branch is composed of neural networks designed to process visual information to produce a vision feature vector  $\mathbf{V}_v$ . The non-vision branch comprises neural networks that generate a non-vision feature vector  $\mathbf{V}_{nv}$  based on non-visual information as input. These two feature vectors are concatenated and provided as input to the attention block of the initial fusion branch. In parallel, the sensor branch processes the time-synchronized motion sensor data and the pedestrian motion direction information to produce the motion sensor feature vector  $\mathbf{V}_s$ . The output of the sensor branch is then fused with the output of the initial fusion branch to make a final prediction about the pedestrian  $i$ ’s action  $A_i^{t+f}$ .

We present the details of each branch. The goal of the non-vision branch is to produce the non-vision feature vector  $\mathbf{V}_{nv}$  using the temporal changes of the trajectory of a pedestrian, the key points of the pedestrian pose, and the ego-vehicle speed as input. More specifically, the pose information is provided to an RNN-based encoder, for which a gated recurrent unit (GRU) (Cho et al. 2014) is adopted since a GRU is known to be more computationally efficient than LSTM. The GRU module consists of 256 hidden units. It outputs a feature tensor of size  $[16, 256]$ , which is then

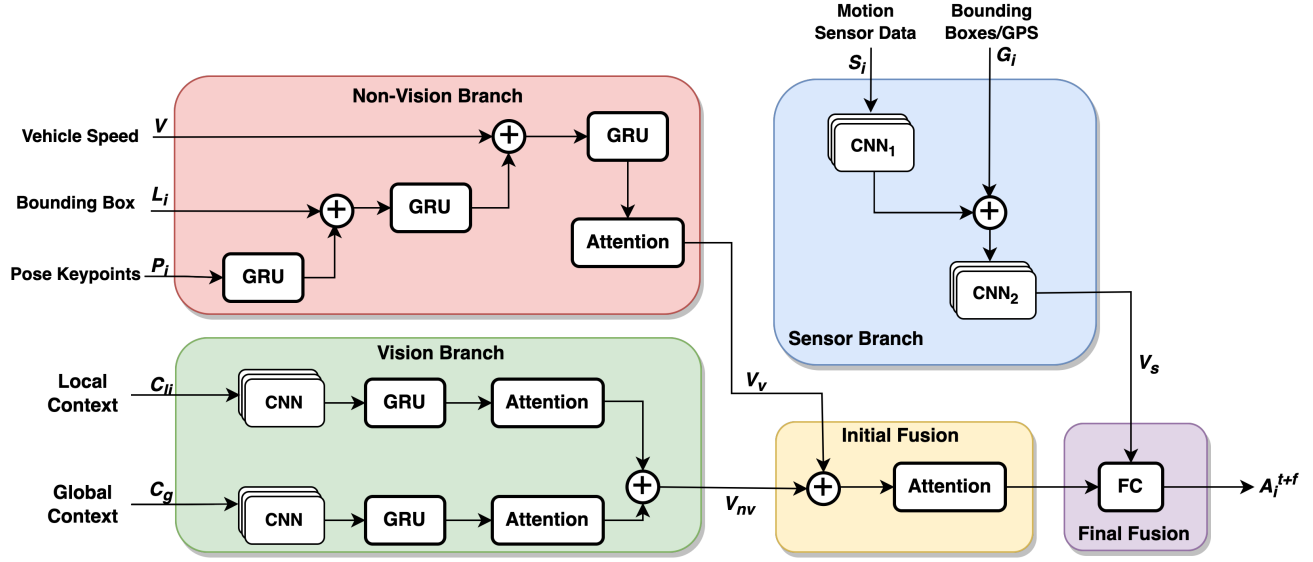


Figure 3: An architecture of the proposed pedestrian intention prediction model. An initial fusion is performed on the feature vectors produced by the non-vision and vision branches, and then the final fusion is performed by integrating with the output of the sensor branch.

concatenated with the bounding box information (*i.e.*, the trajectory information of the pedestrian). The concatenated vector is fed into another GRU module. The output is then concatenated with the vehicle speed information and is provided as input to the last GRU module. The output of the last GRU module is provisioned to the attention block, obtaining the non-vision vector  $\mathbf{V}_{nv}$ .

Similar to the non-vision branch, the vision branch produces the vision feature vector  $\mathbf{V}_v$  using the local and global context as input. The local context represents the pedestrian’s appearance around the bounding box. The global context captures “significant” objects in the semantically segmented scene. More specifically, the local context is processed by extracting spatial features using the CNN module and subsequently capturing the temporal features using the GRU module. For the CNN module, the VGG19 model (Simonyan and Zisserman 2014) trained with the ImageNet dataset (Deng et al. 2009) is adopted. An input to the CNN module is represented as a 4D array [number of observed frames, rows, cols, channels]. Following Yang *et al.*’s work (Yang et al. 2022), the dimension of the array was set to [16,244,244,3]. More precisely, the fourth maxpooling layer of the CNN module extracts the feature map of each local context image in the dimension of [512,14,14]. The pooling layer with a  $14 \times 14$  kernel then performs averaging of the feature map. And then, it is flattened and concatenated, producing the final feature tensor of size [16,512]. The spatial and temporal features for the global context are extracted in a similar manner based on the CNN and GRU modules. These features both for the local and global context are fed into the attention modules, respectively, and then they are concatenated to produce the final vision feature vector  $\mathbf{V}_v$ . The vision feature vector  $\mathbf{V}_v$  is then fused with the

non-vision feature vector  $\mathbf{V}_{nv}$  in the initial fusion branch.

The sensor branch processes the motion sensor data to produce the sensor feature vector  $\mathbf{V}_s$ . This branch is a key component of the proposed model that supports the limited decision making capability of existing vision-based pedestrian intention prediction models. It allows to maintain the high prediction accuracy in adverse situations where the pedestrian is located very far from the ego-vehicle, and the lighting conditions are poor. More specifically, the motion sensor data in the form of a sequence of time-synchronized accelerometer and gyroscope sensor data are provided as input to a CNN module. This CNN module is primarily designed to detect whether the pedestrian is walking or jogging, which is the precursor of the situation where the pedestrian will cross the road. In other words, the CNN module will quickly capture the initial sign of the pedestrian crossing the street. However, only walking or jogging is not enough if we do not incorporate the direction of the pedestrian movement. Therefore, to better predict the pedestrian intention, the output of the CNN module is fused with input features that can be used to infer the moving direction including GPS coordinates and bounding boxes (Note here that, as we explained, these bounding boxes are preprocessed with our algorithm to enhance the detection rate even under very long distances to the pedestrian), and then the fused input features are provided to another CNN module designed to capture the spatial feature related to the pedestrian moving direction. The output of the CNN module is then fused with the output of the initial fusion branch to generate the final expected action of the pedestrian. Detailed parameters for the two CNN modules are presented in the Experimental Setup section.

Table 1: An effect of the distance between the pedestrian and ego-vehicle.

Distance to Pedestrian	Models	Accuracy	AUC	F1-Score	Precision	Recall
Close ( $\sim 20\text{m}$ )	Our Model	0.8902	0.8617	0.9184	0.878	0.9626
	State-of-the-Art (Yang et al. 2022)	0.8593	0.8376	0.893	0.8724	0.9144
Medium (20m $\sim$ 70m)	Our Model	0.7888	0.7888	0.7871	0.7935	0.7807
	State-of-the-Art (Yang et al. 2022)	0.5428	0.5428	0.3871	0.587	0.2888
Far (70m $\sim$ 180m)	Our Model	<b>0.6107</b>	<b>0.7015</b>	<b>0.5745</b>	<b>1</b>	<b>0.403</b>
	State-of-the-Art (Yang et al. 2022)	0.3478	0.5	0	0	0
Average	Our Model	0.7676	0.7817	0.7899	0.879	0.7172
	State-of-the-Art (Yang et al. 2022)	0.6015	0.6453	0.576	0.8182	0.444

Table 2: Parameters for CNN modules of the sensor branch.

	CNN <sub>1</sub>	CNN <sub>2</sub>
Language	Python 3.10.4	Python 3.10.4
Model Type	TensorFlow (2.9.1) Sequential	TensorFlow (2.9.1) Sequential
Frame Size	100	60
Hop Size	50	10
Epochs:	15	100
Test Size	20%	20%
Optimizer	Adam	Adam
Learning Rate	0.001	0.005
Loss	sparse categorical crossentropy	sparse categorical crossentropy

## Experimental Results

We evaluate the performance of the proposed pedestrian intention prediction model compared with a state-of-the-art method (Yang et al. 2022). An experimental setup is presented, followed by the analysis of experimental results measured with varying distances between the pedestrian and ego-vehicle and different levels of lighting conditions.

### Experimental Setup

A workstation equipped with Intel Xeon Gold 5222 Processor, NVIDIA® RTX™ A4000, and 48GB RAM running on Windows 10 OS was used to train and test the proposed model and the state-of-the-art model (Yang et al. 2022). The vision and non-vision branches were implemented based on (Yang et al. 2022). Specifically, a dropout rate of 0.5 was used in the attention module. The L2 regularization of 0.001 was applied for the FC layer, and the Adam optimizer and the binary cross-entropy loss were used. Additionally, the learning rate of  $5 \times 10^{-7}$ , batch size of 2, and 40 epochs were used. Table 2 summarizes parameters selected through extensive trial and error to train the CNN models denoted by CNN<sub>1</sub> and CNN<sub>2</sub> of the sensor branch.

The state-of-the-art model (Yang et al. 2022) was trained using both the JAAD dataset and our dataset. Since the state-of-the-art model does not utilize motion sensor data in making pedestrian intention prediction, the motion sensor data of our dataset were excluded in training the state-of-the-art model. Our model was also trained with the JAAD dataset and our dataset. It is worth to mention that our model

can still make a prediction without motion sensor data enabling training with the JADD dataset. Both models were tested with the same test dataset which is 20% randomly selected video clips from our dataset with varying distances and lighting conditions. The metrics measured in this experiment are the accuracy, AUC, F1-score, precision, and recall. These metrics are selected to provide results that are consistent with existing studies as most of the existing pedestrian prediction solutions and benchmark studies adopt these metrics to report their results (Yang et al. 2022).

### Effect of Distance

We evaluate the performance of our model by varying the distance between the pedestrian and ego-vehicle. We organized the test dataset into close ( $\sim 20\text{m}$ ), medium (20m $\sim$ 70m), and far (70m $\sim$ 180m) in accordance with the distance to the pedestrian. Fig. 4 displays snapshots of the pedestrian at different distances. The results are presented in Table 1. We observed that the accuracy and AUC for the state-of-the-art model degraded as the distance increased from close to far by 59.5% and 40.3%, respectively, exhibiting its weakness when the distance is far due to the unreliability of visual information. Notably, F1-score, precision, and recall for the state-of-the-art model were all 0 when the distance was far, indicating no correctly predicted positive observations.

In contrast to the state-of-the-art model, the results demonstrate that our model is significantly less susceptible to the distance between the pedestrian and ego-vehicle. Although the performance of our model also degraded in terms of the accuracy, AUC, F1-score, and recall as the distance increased, it substantially outperformed the state-of-the-art model regardless of the distance. More specifically, compared with the state-of-the-art model, our model improved the accuracy and AUC by up to 44.3% and 30.7%, respectively; not to mention, the F1-score, precision, and recall of our model are significantly higher when the distance is far since the values of the metrics for the state-of-the-art model were all 0. On average, the proposed model improved the accuracy, AUC, F1-score, precision, and recall by 27.8%, 21%, 37.1%, 7.5%, 61.4%, respectively, compared with the state-of-the-art model.

Another interesting observation was that our model performed slightly better even under the scenarios where the distance was very close, compared with the state-of-the-art model. Specifically, our model improved the accuracy, AUC,

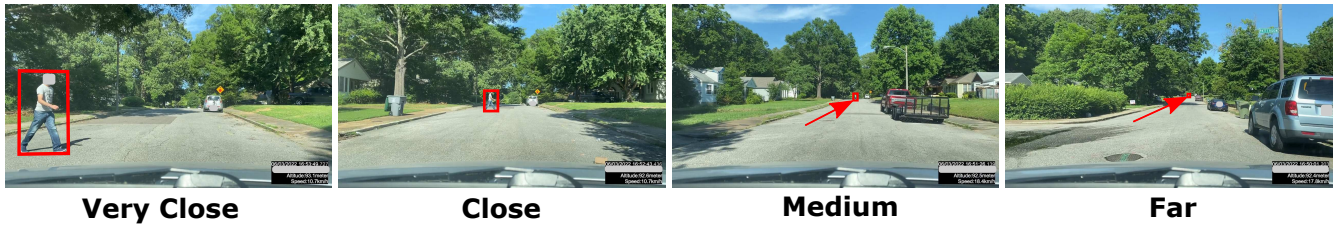


Figure 4: Examples of crossing pedestrians at different distances. Although the pedestrian seems to be far away from the ego-vehicle in the “far” example, it only takes about 9 seconds to reach the pedestrian.

Table 3: An effect of the lighting conditions

Lighting Conditions	Models	Accuracy	AUC	F1-Score	Precision	Recall
Sunny	Our Model	0.6291	0.6265	0.66	0.6306	0.6923
	State-of-the-Art (Yang et al. 2022)	0.5091	0.5111	0.4944	0.5323	0.4615
Cloudy	Our Model	0.7818	0.797	0.7987	0.8947	0.7212
	State-of-the-Art (Yang et al. 2022)	0.6036	0.6485	0.5622	0.8333	0.4242
Rainy	Our Model	0.8727	0.8864	0.9157	0.9744	0.8636
	State-of-the-Art (Yang et al. 2022)	0.7091	0.7841	0.7838	0.9667	0.6591
Night	Our Model	<b>0.803</b>	<b>0.8424</b>	<b>0.8129</b>	<b>1</b>	<b>0.6848</b>
	State-of-the-Art (Yang et al. 2022)	0.625	0.7	0.5714	1	0.4

F1-score, precision, and recall in “close” scenarios by 4.7%, 3.6%, 2.2%, 0.2%, and 5.5%, respectively. A possible explanation is that in some cases the pedestrian pose information was not accurate even if the distance was very close, and the motion sensor data were used to rectify the inaccurate visual information, thereby improving the performance.

### Effect of Lighting Conditions

We analyze the performance of our model compared with the state-of-the-art model by varying the lighting conditions. The test dataset was organized, based on the lighting conditions, into [sunny, cloudy, rainy, night]. The results are summarized in Table 3. Interestingly, we made a counter-intuitive observation. More specifically, we expected that the accuracy for the state-of-the-art model would be lower when the lighting conditions are not good because the model relies on the visual information to make a prediction. Conversely, however, the accuracy for the state-of-the-art model turned out to be higher at night when the lighting conditions are significantly lacking compared to sunny days. We found that the reason was because the state-of-the-art model was not able to make a decision at all due to extremely poor visibility of the pedestrian, and this “no prediction” by the model was counted as a prediction of “not crossing”. As a result, most of the non-crossing actions were considered as being predicted correctly even though the model did not even make a prediction. Due to this counter-intuitive observation, we focused on the recall results since the recall value represents the percentage of correctly predicted events out of all pedestrian-crossing events. In Table 3, the recall results indicate that the performance for the state-of-the-art model actually degraded under poor lighting conditions, *i.e.*, at night and in cloudy conditions.

We made a similar observation for our model. The reason

is because our model also exploits the visual information to make a prediction although the decision is reinforced by incorporating motion sensor data. However, compared with the state-of-the-art model, our model is significantly less susceptible to poor lighting conditions. More specifically, the recall results for our model indicate that our model performs consistently well in all lighting conditions. In particular, the performance degradation in terms of the recall value at night compared with that under the sunny condition was only 1.5%, compared to 13% for the state-of-the-art model. Additionally, we observed that our model achieved higher accuracy, AUC, F1-score, and precision compared with the state-of-the-art model in most lighting conditions. The results demonstrate the significant advantages of integrating with motion sensor data in improving the performance to corroborate the limited decision making capacity of the vision and non-vision branches.

### Conclusions

We have presented a novel pedestrian intention prediction model to address the inherent limitation of state-of-the-art approaches that heavily rely on vision information to make a prediction decision. The proposed model incorporates motion sensor data collected with the pedestrian’s smartwatch to boost the performance when the visual information is not accurate enough, especially when the distance to the pedestrian is far, and the lighting conditions are not sufficient. Additionally, we have performed a large-scale data collection and introduce the first pedestrian intention dataset integrated with time-synchronized motion sensor data. The dataset consists of a total of 128 video clips and is strategically organized according to different distances and lighting conditions aiming to spark research on pedestrian intention prediction solutions based on the motion sensor data. We

have trained and tested our model using the widely adopted JAAD dataset and our own dataset to demonstrate the effectiveness of our model. We validated that compared with a state-of-the-art approach, our model performs significantly better especially in adverse scenarios where the visual information is not accurate due to the long distance and poor lighting conditions

## References

- Alahi, A.; Goel, K.; Ramanathan, V.; Robicquet, A.; Fei-Fei, L.; and Savarese, S. 2016. Social lstm: Human trajectory prediction in crowded spaces. In *Proceedings of the IEEE conference on computer vision and pattern recognition*, 961–971.
- Bartoli, F.; Lisanti, G.; Ballan, L.; and Del Bimbo, A. 2018. Context-aware trajectory prediction. In *2018 24th International Conference on Pattern Recognition (ICPR)*, 1941–1946. IEEE.
- Cadena, P. R. G.; Qian, Y.; Wang, C.; and Yang, M. 2022. Pedestrian Graph+: A Fast Pedestrian Crossing Prediction Model Based on Graph Convolutional Networks. *IEEE Transactions on Intelligent Transportation Systems*.
- Cadena, P. R. G.; Yang, M.; Qian, Y.; and Wang, C. 2019. Pedestrian graph: Pedestrian crossing prediction based on 2d pose estimation and graph convolutional networks. In *2019 IEEE Intelligent Transportation Systems Conference (ITSC)*, 2000–2005. IEEE.
- Cao, Z.; Simon, T.; Wei, S.-E.; and Sheikh, Y. 2017. Realtime multi-person 2d pose estimation using part affinity fields. In *Proceedings of the IEEE conference on computer vision and pattern recognition*, 7291–7299.
- Chaabane, M.; Trabelsi, A.; Blanchard, N.; and Beveridge, R. 2020. Looking ahead: Anticipating pedestrians crossing with future frames prediction. In *Proceedings of the IEEE/CVF Winter Conference on Applications of Computer Vision*, 2297–2306.
- Chen, L.-C.; Papandreou, G.; Schroff, F.; and Adam, H. 2017. Rethinking atrous convolution for semantic image segmentation. *arXiv preprint arXiv:1706.05587*.
- Chen, T.; Tian, R.; and Ding, Z. 2021. Visual reasoning using graph convolutional networks for predicting pedestrian crossing intention. In *Proceedings of the IEEE/CVF International Conference on Computer Vision*, 3103–3109.
- Cho, K.; Van Merriënboer, B.; Bahdanau, D.; and Bengio, Y. 2014. On the properties of neural machine translation: Encoder-decoder approaches. *arXiv preprint arXiv:1409.1259*.
- Cordts, M.; Omran, M.; Ramos, S.; Rehfeld, T.; Enzweiler, M.; Benenson, R.; Franke, U.; Roth, S.; and Schiele, B. 2016. The cityscapes dataset for semantic urban scene understanding. In *Proceedings of the IEEE conference on computer vision and pattern recognition*, 3213–3223.
- Deng, J.; Dong, W.; Socher, R.; Li, L.-J.; Li, K.; and Fei-Fei, L. 2009. Imagenet: A large-scale hierarchical image database. In *2009 IEEE conference on computer vision and pattern recognition*, 248–255. Ieee.
- Fang, Z.; and López, A. M. 2018. Is the pedestrian going to cross? answering by 2d pose estimation. In *2018 IEEE Intelligent Vehicles Symposium (IV)*, 1271–1276.
- Gujjar, P.; and Vaughan, R. 2019. Classifying pedestrian actions in advance using predicted video of urban driving scenes. In *2019 International Conference on Robotics and Automation (ICRA)*, 2097–2103. IEEE.
- Gupta, A.; Johnson, J.; Fei-Fei, L.; Savarese, S.; and Alahi, A. 2018. Social gan: Socially acceptable trajectories with generative adversarial networks. In *Proceedings of the IEEE conference on computer vision and pattern recognition*, 2255–2264.
- Kotseruba, I.; Rasouli, A.; and Tsotsos, J. K. 2020. Do they want to cross? understanding pedestrian intention for behavior prediction. In *2020 IEEE Intelligent Vehicles Symposium (IV)*, 1688–1693. IEEE.
- Kotseruba, I.; Rasouli, A.; and Tsotsos, J. K. 2021. Benchmark for evaluating pedestrian action prediction. In *Proceedings of the IEEE/CVF Winter Conference on Applications of Computer Vision*, 1258–1268.
- Lee, N.; Choi, W.; Vernaza, P.; Choy, C. B.; Torr, P. H.; and Chandraker, M. 2017. Desire: Distant future prediction in dynamic scenes with interacting agents. In *Proceedings of the IEEE conference on computer vision and pattern recognition*, 336–345.
- Liu, B.; Adeli, E.; Cao, Z.; Lee, K.-H.; Sheno, A.; Gaidon, A.; and Niebles, J. C. 2020. Spatiotemporal relationship reasoning for pedestrian intent prediction. *IEEE Robotics and Automation Letters*, 5(2): 3485–3492.
- Lorenzo, J.; Alonso, I. P.; Izquierdo, R.; Ballardini, A. L.; Saz, Á. H.; Llorca, D. F.; and Sotelo, M. Á. 2021. CAP-former: pedestrian crossing action prediction using transformer. *Sensors*, 21(17): 5694.
- Lorenzo, J.; Parra, I.; Wirth, F.; Stiller, C.; Llorca, D. F.; and Sotelo, M. A. 2020. Rnn-based pedestrian crossing prediction using activity and pose-related features. In *2020 IEEE Intelligent Vehicles Symposium (IV)*, 1801–1806. IEEE.
- Malla, S.; Dariush, B.; and Choi, C. 2020. Titan: Future forecast using action priors. In *Proceedings of the IEEE/CVF Conference on Computer Vision and Pattern Recognition*, 11186–11196.
- Neogi, S.; Hoy, M.; Chaoqun, W.; and Dauwels, J. 2017. Context based pedestrian intention prediction using factored latent dynamic conditional random fields. In *2017 IEEE Symposium Series on Computational Intelligence (SSCI)*, 1–8. IEEE.
- Piccoli, F.; Balakrishnan, R.; Perez, M. J.; Sachdeo, M.; Nunez, C.; Tang, M.; Andreasson, K.; Bjurek, K.; Raj, R. D.; Davidsson, E.; et al. 2020. Fussi-net: Fusion of spatio-temporal skeletons for intention prediction network. In *2020 54th Asilomar Conference on Signals, Systems, and Computers*, 68–72. IEEE.
- Quintero, R.; Parra, I.; Lorenzo, J.; Fernández-Llorca, D.; and Sotelo, M. 2017. Pedestrian intention recognition by means of a hidden markov model and body language. In *2017 IEEE 20th international conference on intelligent transportation systems (ITSC)*, 1–7. IEEE.



- Rasouli, A.; Kotseruba, I.; Kunic, T.; and Tsotsos, J. K. 2019. Pie: A large-scale dataset and models for pedestrian intention estimation and trajectory prediction. In *Proceedings of the IEEE/CVF International Conference on Computer Vision*, 6262–6271.
- Rasouli, A.; Kotseruba, I.; and Tsotsos, J. K. 2017. Are they going to cross? a benchmark dataset and baseline for pedestrian crosswalk behavior. In *Proceedings of the IEEE International Conference on Computer Vision Workshops*, 206–213.
- Rasouli, A.; Kotseruba, I.; and Tsotsos, J. K. 2020. Pedestrian action anticipation using contextual feature fusion in stacked rnns. *arXiv preprint arXiv:2005.06582*.
- Rasouli, A.; Rohani, M.; and Luo, J. 2021. Bifold and Semantic Reasoning for Pedestrian Behavior Prediction. In *Proceedings of the IEEE/CVF International Conference on Computer Vision*, 15600–15610.
- Rasouli, A.; and Tsotsos, J. K. 2018. Joint attention in driver-pedestrian interaction: from theory to practice. *arXiv preprint arXiv:1802.02522*.
- Rasouli, A.; Yau, T.; Rohani, M.; and Luo, J. 2020. Multi-modal hybrid architecture for pedestrian action prediction. *arXiv preprint arXiv:2012.00514*.
- Razali, H.; Mordan, T.; and Alahi, A. 2021. Pedestrian intention prediction: A convolutional bottom-up multi-task approach. *Transportation research part C: emerging technologies*, 130: 103259.
- Sadeghian, A.; Kosaraju, V.; Sadeghian, A.; Hirose, N.; Rezatofghi, H.; and Savarese, S. 2019. Sophie: An attentive gan for predicting paths compliant to social and physical constraints. In *Proceedings of the IEEE/CVF conference on computer vision and pattern recognition*, 1349–1358.
- Saleh, K.; Hossny, M.; and Nahavandi, S. 2019. Real-time intent prediction of pedestrians for autonomous ground vehicles via spatio-temporal densenet. In *2019 International Conference on Robotics and Automation (ICRA)*, 9704–9710. IEEE.
- Simonyan, K.; and Zisserman, A. 2014. Very deep convolutional networks for large-scale image recognition. *arXiv preprint arXiv:1409.1556*.
- Singh, A.; and Suddamalla, U. 2021. Multi-Input Fusion for Practical Pedestrian Intention Prediction. In *Proceedings of the IEEE/CVF International Conference on Computer Vision*, 2304–2311.
- Wojke, N.; and Bewley, A. 2018. Deep cosine metric learning for person re-identification. In *2018 IEEE winter conference on applications of computer vision (WACV)*, 748–756. IEEE.
- Yang, B.; Zhan, W.; Wang, P.; Chan, C.; Cai, Y.; and Wang, N. 2021. Crossing or Not? Context-Based Recognition of Pedestrian Crossing Intention in the Urban Environment. *IEEE Transactions on Intelligent Transportation Systems*.
- Yang, D.; Zhang, H.; Yurtsever, E.; Redmill, K.; and Ozguner, U. 2022. Predicting pedestrian crossing intention with feature fusion and spatio-temporal attention. *IEEE Transactions on Intelligent Vehicles*.
- Zhang, S.; Abdel-Aty, M.; Wu, Y.; and Zheng, O. 2021. Pedestrian crossing intention prediction at red-light using pose estimation. *IEEE Transactions on Intelligent Transportation Systems*.
- Zhao, S.; Li, H.; Ke, Q.; Liu, L.; and Zhang, R. 2021. Action-ViT: Pedestrian Intent Prediction in Traffic Scenes. *IEEE Signal Processing Letters*, 29: 324–328.